Inhibition of Oxide Formation on Aluminum Nanoparticles by Transition Metal Coating

Timothy J. Foley,* Curtis E. Johnson, and Kelvin T. Higa

NAVAIR, Weapons Division, 1 Administration Circle, China Lake, California 93555

Received November 26, 2004. Revised Manuscript Received June 6, 2005

Nanometer-sized aluminum powder was synthesized by thermal decomposition of an alane solution in the presence of a titanium catalyst under an inert atmosphere. The resulting material, formally devoid of an oxide layer, was used to reduce complexes of gold, nickel, palladium, and silver. The reduction process yielded materials that contained the transition metal at a level between 1 and 3 atom % on a metals basis, as determined by inductively coupled plasma atomic emission spectroscopy and energy dispersive spectroscopy. After exposure to air at ambient conditions, the transition metal treated aluminum materials were found to contain less aluminum oxide than an aluminum sample that was not treated with a transition metal. The nickel treated sample contained as much or more metallic aluminum as the untreated aluminum sample, indicating that the passivating layer in the nickel treated aluminum was highly efficient at protecting the underlying aluminum.

1. Introduction

Properties of nanometer-scaled aluminum particles can differ substantially from those observed in larger sized samples. Aluminum nanoparticles are more reactive than micrometer-sized particles toward oxidation and other reactions as a result of high specific surface area.[1] While nano-Al has interesting and useful properties, it also has a size-related limitation due to the oxide layer that rapidly forms when aluminum surfaces are exposed to air. The oxide layer is approximately 2−5 nm thick, and the weight percent of oxide increases as the particle diameter decreases.[2] For an air-passivated 30-nm Al particle about half of the weight is aluminum oxide. The oxide generally does not constructively contribute to the uses for the metal and is often considered "dead weight", whose reduction or elimination would enhance the usefulness of the material. As an example, if the amount of active aluminum in a nano-aluminum powder is increased 5 wt % this corresponds to an additional 1.55 kJ/g of potential chemical energy, based on the conversion of metal to metal oxide.

An alternative passivation approach to the usual aluminum oxide layer is to coat aluminum with other metals or metal oxides. Conceivably, very thin layers of these materials could be more effective at passivating the aluminum than aluminum oxide. Unlike aluminum oxide, these metal or metal oxide coatings could contribute to the reactivity of aluminum at elevated temperatures. The coating metal could undergo intermetallic reactions with the underlying aluminum, while metal oxides could undergo thermite reactions.[3] While it is expected that this will spontaneously occur at the interface of the aluminum and the coated material after some solid-state limited diffusion distance, these reactions will be arrested. Additionally, coatings of nickel and other metals have been studied on micrometer-sized aluminum powders and have been found to enhance ignition and combustion behavior.[4]

Although the aluminum oxide passivation layer is undesirable in many uses of aluminum, this thin layer is very efficient at stabilizing the otherwise highly reactive aluminum surface. There has been little reported success in alternative passivation schemes. Generally, either the passivating layer is less effective, or more material on a weight or volume basis is required to achieve the same protective effect. Passivation of aluminum powder using stearic acid has been known to give a material with higher active (metallic) aluminum content than the corresponding air-passivated material.[5]

To study alternative passivation approaches for Al nanoparticles requires a material with a surface free of aluminum oxide. A solution method was chosen as the most convenient

* To whom correspondence should be addressed. E-mail: timothy.foley@navy.mil.

(1) (a) Auman, C. E.; Skofronick, G. L.; Martin, J. A. *J. Vac. Sci. Technol. B* **1995**, *13*, 1178. (b) DeSena, J. T.; Kuo, K. K. *J. Propul. Power* **1999**, *15*, 794. (c) Yang, Y.; Sun, Z.; Wang, S.; Dlott, D. D. *J. Phys. Chem. B* **2003**, *107*, 4485.

(2) (a) *Aluminum: Properties and Physical Metallurgy*; Hatch, J. E., Ed.; American Society for Metals: Metals Park, OH, 1984. (b) *Corrosion of Aluminum and Aluminum Alloys*; Davis, J. R., Ed.; ASM International: Materials Park, OH, 1999. (c) Sanchez-Lopez, J. C.; Gonzalez-Elipe, A. R.; A.; Fernandez, A. *J. Mater. Res.* **1998**, *13*, 703. (d) Smith, B. L.; Jorgensen, B. S.; Busse, J. R.; Ferris, M. J.; Danen, W. C. *Determination of Oxide Layer Thickness of Aluminum Nanopartricles*; Report LA-UR-01-1665; Los Alamos National Laboratories: Los Alamos, NM, 2001.

(3) (a) Wang, L. L.; Munir, Z. A.; Maximov, Y. M. *J. Mater. Sci.* **1993**, *28*, 3693. (b) Hardt, A. P.; Phung, P. V. *Combust. Flame* **1973**, *21*, 77.

(4) (a) Yagodnikov, D. A.; Voronetskii, A. V. *Combust., Explos. Shock Waves* **1997**, *33*, 49. (b) Shafirovich, E.; Mukasyan, A.; Thiers, L.; Varma, A.; Legrand, B.; Chauveau, C.; Gokalp, I. *Combust. Sci. Technol.* **2002**, *174*, 125.

(5) (a) Lyashko, A. P.; Ilyin, A. P.; Savelev, G. G. *Russ. J. Appl. Chem.* **1993**, *66*, 999. (b) Kwon, K.; Gromov, A. A.; Ilyin, A. P.; Rin, G. *Appl. Surf. Sci.* **2003**, *211*, 57. (c) Jouet, R. J.; Warren, A. D.; Rosenberg, D. M.; Belitto, V. J.; Park, K.; Zachariah, M. R. *Chem. Mater.* **2005**, *17*, 2987.

10.1021/cm047931k
Published on Web 07/14/2005

route to preparing oxide-free aluminum nanoparticles. In this process tertiary amine adducts of alane are thermally decomposed in the presence of a titanium catalyst.[6] Because the reaction is run under an inert atmosphere, the aluminum generated by this process is formally devoid of an oxide passivation layer and is ideal for studying the effects of surface modifications on the subsequent formation of aluminum oxide. Controlling the initial concentration of the titanium catalyst in the reaction solution, limits the nucleation sites allowing particle sizes ranging from 50 to 500 nm to be controllably produced.

2. Experimental Section

2.1. Synthesis. The triethylamine adduct of alane ($AlH_3 \cdot NEt_3$) was prepared in heptane solution using a modification of a procedure described for alane dimethylethylamine.[7] All other reagents were purchased from Aldrich and were used as received. Solvents were purchased from Aldrich and were treated according to literature procedures[8] to render them anhydrous and oxygen free. Sample manipulation prior to air passivation was performed under an atmosphere of argon. The percent yields reported with the syntheses of the samples are derived from the starting mass of the unpassivated materials and the expected mass of the coated materials assuming complete consumption of the coating reagent and that the samples were pure metal. This simplification does not take into account the likelihood that organic species are ligated onto the surface of the particles. Therefore, yields are not quantitative and are presented for comparative purposes only.

Care should be exercised when handling Al nanopowders before or after air passivation, as they can be pyrophoric and can be readily ignited by electrostatic discharge.

Synthesis of "Unpassivated" Aluminum Powder. Neat titanium isopropoxide (0.579 g, 2.04 mmol) and 20 mL of NEt_3 were added to a Schlenk flask, after which the solution was heated to 70 °C. To the rapidly stirred solution was added 150 mL of a 1.5 M heptane solution of $AlH_3 \cdot NEt_3$ in a dropwise fashion over the course of several minutes. A brown precipitate formed immediately with a concurrent evolution of gas. This reaction ceased within 2 min of the initial addition and no reaction was evident for the following 10 min. Following this induction period the solution darkened and the walls of the reaction flask became covered with a metallic mirror. Gas production was again evident, continuing for approximately 10 min as a dark precipitate formed. Reaction conditions were maintained for an additional hour after gas evolution was no longer evident to ensure completeness of the reaction. Subsequently, the flask was cooled and the powder allowed to settle. The liquid was decanted and the product was washed three times with dimethoxyethane (DME). Decantation and washing of the material were achieved by the use of a filter cannula. The supernatant liquid from the first decantation was colorless, but the subsequent washings with DME yielded solutions that were darkly colored. Coloration of the organic wash was in all likelihood due to suspended Al nanoparticles. Volatile species were then removed in vacuo at room temperature, providing 4.50 g of product (0.167 mol, 75% based on pure Al). This material was stored in a glovebox under inert atmosphere.

Synthesis of Palladium-Coated Aluminum Powder ((Al)Pd). A portion of the aluminum powder described above (0.500 g, 18.5 mmol) was slurried with 20 mL of DME. In a separate flask, palladium(II) acetylacetonate (0.114 g, 0.375 mmol) was dissolved in DME (20 mL). The yellow palladium solution was added to the stirred aluminum slurry and allowed to react at room temperature for 12 h. Afterward, the stirring was halted, the aluminum allowed to settle and the reaction solvent decanted. Decantation of the reaction solution and washing of the product did not afford a darkly colored solution as observed in the aluminum powder synthesis. The resulting solid was then washed three times with DME, and dried in vacuo at room temperature, to yield 0.531 g of (Al)Pd (98% of predicted weight).

Synthesis of Silver-Coated Aluminum Powder ((Al)Ag). The silver-coated sample was generated by the procedure used to produce (Al)Pd. In this experiment 0.078 g of silver(I) acetylacetonate (0.375 mmol) and 0.500 g of Al (18.5 mmol) were used. This yielded 0.538 g of (Al)Ag (99% of predicted weight).

Synthesis of Gold-Coated Aluminum Powder ((Al)Au). The gold-coated material was produced in the same fashion as (Al)Pd, utilizing 0.110 g of gold(I) chloride dimethyl sulfide (0.375 mmol) and 0.500 g of Al (18.5 mmol). This yielded 0.523 g of (Al)Au (91% of predicted weight).

Synthesis of Nickel-Coated Aluminum Powder ((Al)Ni). This material was generated by the procedure used to produce (Al)Pd utilizing 0.096 g of nickel(II) acetylacetonate (0.375 mmol) and 0.500 g of Al (18.5 mmol). This yielded 0.46 g of (Al)Ni (88% of predicted weight)

Air Passivation of Samples. Approximately 0.250 g of a sample was placed in a glass vial; the vial was then capped and removed from the glovebox. A pinhole was made in the cap to allow the gradual displacement of the argon over the sample with air. After standing for 24 h the samples were safe to manipulate. Shorter periods of passivation tended to produce materials that would spontaneously ignite on removal from the vial.

2.2. Characterization. Analyses were performed on materials following air passivation. Samples were digested in accord with Environmental Protection Agency (EPA) method 3050 B,[9] and inductively coupled plasma atomic emission spectroscopy (ICP-AES) was performed under the guidelines of EPA method 6010 B.[9] X-ray powder diffraction experiments (Cu Kα) were performed on a Scintag Pad 5 diffractometer. Spectra were collected at a step rate of 0.04°/min and were scanned from 5 to 120°. Scanning electron microscopy (SEM) was conducted on an Electroscan Environmental model E-3 microscope in the presence of water vapor at ~5 Torr, and on an Amray model 1400 instrument. Surface area analysis was conducted on a Quantachrome Autosorb-1 instrument using nitrogen adsorption and analysis according to the Brunauer, Emmett, and Teller (BET) method.[10] Samples were degassed under vacuum at 100 °C for 30 min prior to analysis. Each analysis is based on the data for three runs which were averaged for each sample. Thermogravimetric analysis was performed on a TA Instruments 2950 Thermogravimetric Analyzer under an air flow of 40 mL/min. Sample weights ranged from 2 to 7 mg and weight data were corrected for the instrumental baseline response, based on blank (empty aluminum oxide pan) experiments.

2.3. Composition Calculations. The weight gain upon oxidation was used to calculate a range of possible compositions for the samples, reflecting the uncertainty in the oxidation state of Ti and the coating metal. The composition of the samples before oxidation is calculated for two limiting cases: one in which weight gain is

(6) Higa, K. T.; Johnson, C. E.; Hollins, R. A. U.S. Patent 5,885,321, 1999.
(7) Frigo, D. M.; van Eijden, J. M. *Chem. Mater*. **1994**, *6*, 190.
(8) Armarego, W. L. F.; Perrin, D. D. *Purification of Laboratory Chemicals*, 4th ed.; Butterworth-Heinemann: Woburn, MA, 1996.
(9) Environmental Protection Agency publication SW-846 Update III, Chapter 3. http://www.epa.gov/epaoswer/hazwaste/test/pdfs/chap3.pdf (accessed Nov 2002).
(10) Brunauer, S.; Emmett, P. H.; Teller, E. *J. Am. Chem. Soc*. **1938**, *60*, 309.

Table 1. Characterization of Metal-Coated Aluminum Powders

sample	component	ICP-AES mol % vs Al	EDS mol % vs Al	BET surface area, m^2/g	BET size, nm	SEM size, nm	TGA min., wt %	TGA max., wt %
Al	titanium	1.55	1.1			150	95.2	154.7
(Al)Pd	palladium	1.62	2.1	26.7	83	150	97.6	157.5
	titanium	1.15	1.2					
(Al)Ag	silver	*a*	1.9	28.9	77	150	97.4	157.9
	titanium	1.22	1.1					
(Al)Au	gold	1.24	2.4	15.2	146	150	97.2	155.8
	titanium	1.26	1.1					
(Al)Ni	nickel	2.41	1.8	28.4	78	150	97.2	160.0
	titanium	1.12	0.8					

[a] Incomplete digestion of this sample resulted in inaccurate ICP-AES analysis for Ag.

based on the oxidation of the Al, the coating metal, and titanium and where it is due solely to Al with the other metals being completely oxidized (e.g., TiO_2, NiO); examples are shown in eqs 1 and 2, with respect to the two circumstances.

$$2X\mathrm{Al} + Y\mathrm{Ni} + Z\mathrm{Ti} + (3X/2 + Y/2 + Z)\mathrm{O}_2 \rightarrow X\mathrm{Al}_2\mathrm{O}_3 + Y\mathrm{NiO} + Z\mathrm{TiO}_2 \quad (1)$$

$$2X\mathrm{Al} + (3X/2)\mathrm{O}_2 \rightarrow X\mathrm{Al}_2\mathrm{O}_3 \quad (2)$$

The calculated compositions are based on the weight gain after volatiles are thermolyzed (i.e., at or before 350 °C). For the general case of conversion to metal oxide products, two equations can be defined which relate the constituents of each sample (eqs 3 and 4).

$$W_{\mathrm{Al}} + W_{\mathrm{Ti}} + W_{\mathrm{M}} + W_{\mathrm{Al_2O_3}} + W_{\mathrm{TiO_2}} + W_{\mathrm{MO}} = 1 \quad (3)$$

$$R = W_{\mathrm{Al}}\phi_{\mathrm{Al}} + W_{\mathrm{Ti}}\phi_{\mathrm{Ti}} + W_{\mathrm{M}}\phi_{\mathrm{M}} + W_{\mathrm{Al_2O_3}} + W_{\mathrm{TiO_2}} + W_{\mathrm{MO}} \quad (4)$$

The first equation details the relative composition of a material. In the second, the relationship between the composition and the observed weight gain due to oxidation is presented. In these equations, W is the weight fraction of the component in a sample as determined by elemental analysis. The subscripts refer to each element with M as the coating metal and MO as the oxide of the coating metal. Summation of the fractional amounts of each constituent is made to equal 1. In the second equation, R is the ratio of the final weight to the minimum weight as determined experimentally by TGA, and ϕ represents the ratio of the formula weight of a metal oxide to the product of the number of moles of metal in the metal oxide and the atomic weight of the metal.

Under the constraints of the first limit, where $W_{\mathrm{TiO_2}} = W_{\mathrm{MO}} = 0$, solving eq 1 for $W_{\mathrm{Al_2O_3}}$, then substituting for this term in eq 2 and rearranging terms to solve for the weight fraction of aluminum metal, gives eq 5.

$$W_{\mathrm{Al}} = [R - 1 - W_{\mathrm{Ti}}(\phi_{\mathrm{Ti}} - 1) - W_{\mathrm{M}}(\phi_{\mathrm{M}} - 1)]/(\phi_{\mathrm{Al}} - 1) \quad (5)$$

In the other case, where $W_{\mathrm{Ti}} = W_{\mathrm{M}} = 0$, the same manipulation leads to the expression in eq 6 for the weight percent of aluminum metal.

$$W_{\mathrm{Al}} = (R - 1)/(\phi_{\mathrm{Al}} - 1) \quad (6)$$

For a metal where the oxide is unstable at 850 °C, the coating metal no longer contributes to the weight gain, while the oxide of the coating metal experiences a loss in weight (example eq 7).

$$2X\mathrm{Al} + Y\mathrm{AgO} + ((3X - \mathrm{Y})/2)\mathrm{O}_2 \rightarrow X\mathrm{Al}_2\mathrm{O}_3 + Y\mathrm{Ag} \quad (7)$$

In this case, eqs 4a−6a were used.

$$R = W_{\mathrm{Al}}\phi_{\mathrm{Al}} + W_{\mathrm{Ti}}\phi_{\mathrm{Ti}} + W_{\mathrm{M}} + W_{\mathrm{Al_2O_3}} + W_{\mathrm{TiO_2}} + W_{\mathrm{MO}}(\phi_{\mathrm{M}}{}^{-1}) \quad (4a)$$

$$W_{\mathrm{Al}} = [R - 1 - W_{\mathrm{Ti}}(\phi_{\mathrm{Ti}} - 1)]/(\phi_{\mathrm{Al}} - 1) \quad (5a)$$

$$W_{\mathrm{Al}} = [R - 1 - W_{\mathrm{MO}}(\phi_{\mathrm{M}}{}^{-1} - 1)]/(\phi_{\mathrm{Al}} - 1) \quad (6a)$$

Utilizing the equations above, in conjunction with the experimentally determined weight gains and compositions of the samples (i.e., mole ratio of Ti and coating metal to Al from ICP-AES data), the overall ranges for the active aluminum content can be calculated.

3. Results and Discussion

3.1. Synthesis and Elemental Analysis. To modify the surface of the aluminum particles, various metals were deposited using soluble salts that were reduced by the aluminum powder. Experiments focused on low loadings of the intended passivating metals. The reduction/deposition was performed in the following manner. Aluminum powder was prepared by the solution method and partitioned into five equal portions. Four of these samples were slurried in dimethoxyethane solutions having 2 mole percent of one of the following complexes: $Pd(acac)_2$, Ag(acac), $AuCl{\cdot}SMe_2$, or $Ni(acac)_2$ (acac = acetylacetonate). The fifth sample of the aluminum was subjected to the same experimental conditions, except that the organic solvent did not contain a transition metal complex. The expected products of the reaction are aluminum powder coated with a zerovalent metal and $Al(acac)_3$ or $AlCl_3$ both of which are soluble in DME. After washing and drying, the samples were exposed to the ambient atmosphere and analyzed for their composition.

The metal content of the samples was determined by two independent methods, ICP-AES and energy dispersive spectroscopy (EDS). According to the analysis, results shown in Table 1, the composition of the samples varied from 1.2 to 2.4 and from 1.9 to 2.4 mol % of the coating metal (relative to the amount Al) by AES and EDS, respectively. From the AES data, Ni was deposited in the largest quantity at 2.4 mol % and Au in the lowest quantity at 1.2 mol %. Titanium originates from the catalyst used in the synthesis of the Al powder, and was present at approximately 1 mol % for all treated samples according to both analysis techniques.

3.2. SEM and BET Measurements. To characterize the size and surfaces of the particles, scanning electron micros-

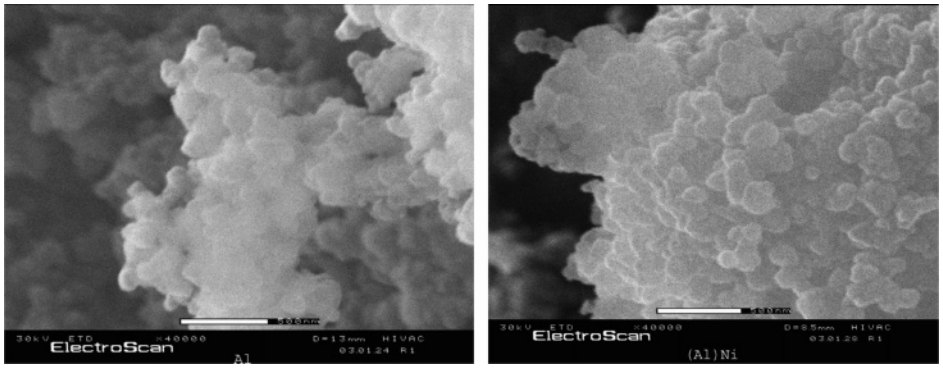

Figure 1. Scanning electron micrographs of Al (left) and (Al)Ni (right) powders. The white bar corresponds to 500 nm.

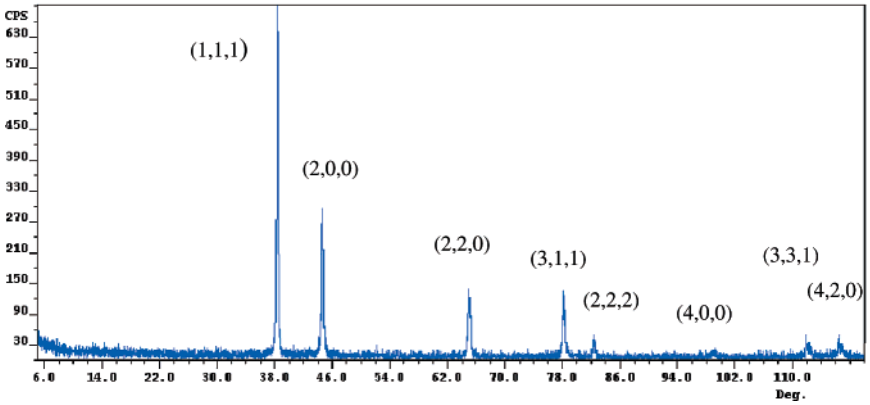

Figure 2. X-ray powder diffraction pattern for (Al)Ni powder. Peak assignments are based on powder diffraction reference code 00-0004-0787.

copy (SEM) and surface area analysis (using the Brunauer−Emmett−Teller (BET) method) were performed on the samples. Electron micrographs reveal that the constituting particles appear to be approximately 150 nm in size and are strongly aggregated together. No variation in the morphology or topology is apparent between samples. As examples, micrographs of Al and (Al)Ni are presented for inspection in Figure 1. Aggregation behavior observed in these samples is not particular to this synthetic method and has been reported for Al nanoparticles produced by other methods.[11] However, the aggregation of the samples produced in this investigation appears to be more severe than in most cases.

Using the surface area per gram as determined by the BET method, an idealized particle size can be calculated based on uniform spherical particles. These results are reported in Table 1. The Pd, Ag, and Ni treated samples have approximately the same specific surface area. The gold sample appears to have half of the surface area and therefore twice the calculated diameter. When BET sizes are compared to the estimated SEM values, only the gold treated sample shows good agreement; for the other samples the BET sizes are smaller by a factor of about two. Differences between the BET and SEM sizes are currently attributed to surface features that are beyond the resolution of the SEM.

3.3. Powder Diffraction. Shown in Figure 2 is the X-ray powder diffraction pattern of (Al)Ni. The peaks are slightly broadened, as is typically observed with nanocrystalline materials. All observed peaks correspond directly to Al metal. Absent from the pattern are peaks for Ni or NiO; this is not a reflection of the quantity of the materials that may be present but only of its crystallinity. In theory the material could be completely composed of an amorphous material and no diffraction pattern would be observed. Diffraction patterns for the other samples were similar, with no peaks observed for the coating metal.

3.4. Thermogravimetric Analysis. Thermogravimetric analysis was conducted in air to provide information on the composition and reactivity of the coated samples relative to the uncoated material (Figure 3). The weight gain is primarily due to oxidation of Al metal with oxygen or water. Care must be taken that the samples do not gain weight too rapidly as this leads to self-heating and ignition. Ignition can lead to the formation of aluminum nitride and oxynitrides, complicating analysis of the weight gain.[12] Slowing the heating rate moderates the rate of weight gain, preventing this possibility. Samples were heated at 20 °C/min from room temperature to 350 °C, 5 °C/min from 350 to 600 °C, and 20°/min from 600 to 850 °C. The temperature was maintained at 850 °C for 4 h to ensure complete oxidation.

Weight changes for the samples can be divided into three regions, consisting of initial weight loss followed by weight gain in two distinct steps. Initially, the samples lose from 2.4 to 4.8% of their weight due to the volatilization of surface

(11) (a) Dufaux, D. P.; Axelbaum, R. L. *Combust. Flame* **1995**, *100*, 350. (b) Il'in, A. P.; Popenko, E. M.; Gromov, A. A.; Shamina, Y. Y.; Tikhonov, D. V. *Combust., Explos. Shock Waves* **2002**, *38*, 665.

(12) (a) Schevchenko, V. G.; Kononenko, V. I.; Latosh, I. N.; Chupova, I. A.; Lukin, N. V. *Combust., Explos. Shock Waves* **1994**, *30*, 635. (b) Il'in, A. P.; Yablunoskii, G. V.; Gromov, A. A.; Popenko, E. M.; Bychin, N. V. *Combust., Explos. Shock Waves* **1999**, *35*, 656. (c) Il'in, A. P.; Proskurovskaya, L. T. *Combust., Explos. Shock Waves* **1990**, *26*, 190. (d) Bucher, P.; Yetter, R. A.; Dryer, F. L.; Vicenzi, E. P.; Parr, T. P.; Hanson-Parr, D. M. *Combust. Flame* **1999**, *117*, 351.

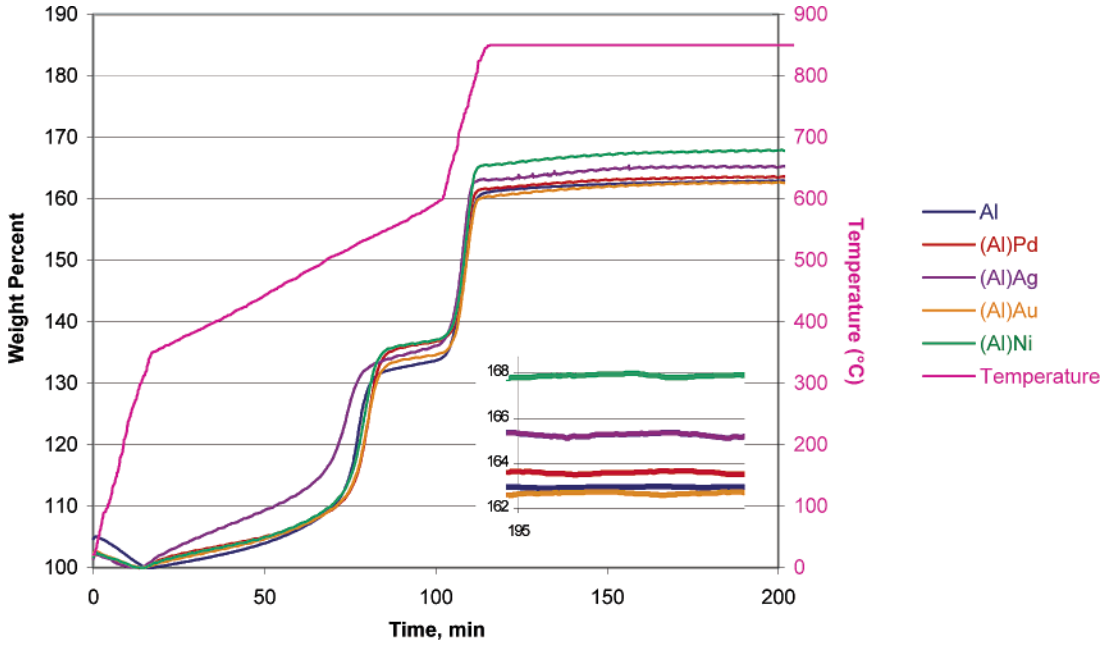

Figure 3. Thermogravimetric analysis of metal-coated aluminum samples under an atmosphere of air. The weight is normalized to the minimum weight. The inset shows an expanded view of the final weight gains.

adsorbed species such as organic species and water; this is essentially completed before the samples reach 350 °C (Figure 3). Following the desorption process, samples begin to gain weight until nearly leveling off at ~550 °C. This corresponds to the oxide skin on the particles thickening and providing a kinetic barrier to further weight gain.[13] Further sample oxidation is curbed until 700 °C, after which the rate increases sharply. The baseline-corrected minimum and maximum weights from the TGA experiments are listed in Table 1.

Initially, a few differences between the samples are easily observed. The Al sample has the largest initial weight loss, indicating that it has the most adsorbed surface species. The silver-coated aluminum, (Al)Ag, has the earliest onset temperature for weight gain, but after the first oxidation step the weight gain profile is similar to those of the other samples. The (Al)Ni and (Al)Pd samples both have higher first step weight gains compared to the Al metal, and the (Al)Ni sample has the highest total weight gain.

3.5. Composition Analysis. The key measure for assessing passivation approaches is the active or metallic aluminum content of the sample. For samples containing only aluminum and aluminum oxide, the weight gain upon complete conversion to aluminum oxide provides a quantitative measure of active aluminum content. However, the oxidation states of the coating metal and Ti are not known. Therefore, only a range of possible active aluminum content can be calculated using the weight gain during oxidation and the amounts of the transition metals in the samples. The composition of the samples before oxidation is calculated for two limiting cases: one where the Ti and coating metal are zerovalent and one where they are completely oxidized (e.g., TiO_2, NiO). While the presence of significant amounts of oxides of the other coating metals (Ag, Au, Pd) is questionable,

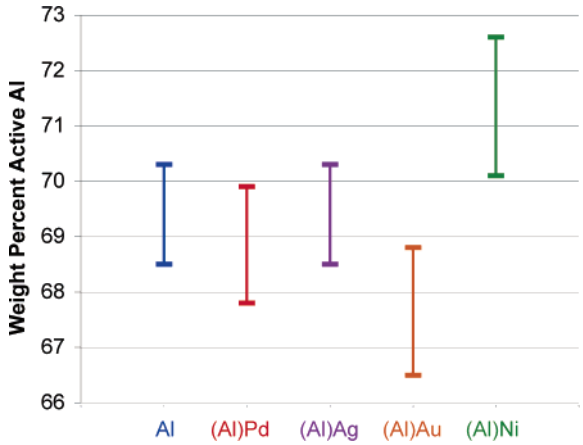

Figure 4. Calculated ranges for the weight percent of aluminum metal in the samples, based on analysis of TGA and ICP-AES data.

this case was included for comparison to the results for Ni. The calculated compositions are based on the material after volatiles are removed during the initial weight loss (i.e., at 350 °C). Note that any oxides of Ag or Au would have decomposed to the elements during heating to 350 °C, while palladium oxides should be essentially decomposed to the elements by 850 °C.[14]

The compositional ranges for each of the samples are presented in Figure 4. The nickel-coated sample has 0−4% more active aluminum than the untreated sample. For the other coated samples the active aluminum content was about the same as that in the uncoated sample. The active aluminum content is generally likely to be near the low end of the range, favoring the reduced forms of Ti and the coating metals. An exception is the nickel sample where the nickel coating is probably mostly oxidized.

(13) Blackburn, P. E.; Gulbransen, E. A. *J. Electrochem. Soc.* **1960**, *107*, 944.

(14) *CRC Handbook of Chemistry and Physics*, 78th ed.; Lide, D. R., Frederikse, H. P. R., Eds.; CRC Press: New York, 1997; pp 4-60, 4-75, and 4-84.

Table 2. Calculated Composition after Loss of Volatiles for Two Limiting Cases of Oxidation States of the Minor Metal Components

sample	oxidation state	wt % active Al	wt % Al_2O_3	wt % Ti	wt % TiO_2	wt % M[a]	wt % MO[a]
Al	$Ti^0 = Ti^{IV}$	68.5	29.2	2.3			
Al	$Ti^{IV} = Ti^{IV}$	70.3	25.9		3.8		
(Al)Pd	$Pd^0/Ti^0 = Pd^0/Ti^{IV}$	67.8	25.4	1.7		5.2	
(Al)Pd	$Pd^{II}/Ti^{IV} = Pd^0/Ti^{IV}$	69.9	21.4		2.8		6.0
(Al)Ag	$Ag^0/Ti^0 = Ag^0/Ti^{IV}$	68.5	23.6	1.8		6.2	
(Al)Ag	$Ag^I/Ti^{IV} = Ag^0/Ti^{IV}$	70.3	20.1		2.9		6.6
(Al)Au	$Au^0/Ti^0 = Au^0/Ti^{IV}$	66.5	24.6	1.8		7.2	
(Al)Au	$Au^{III}/Ti^{IV} = Au^0/Ti^{IV}$	68.8	20.2		3.0		8.1
(Al)Ni	$Ni^0/Ti^0 = Ni^{II}/Ti^{IV}$	70.1	24.0	1.6		4.3	
(Al)Ni	$Ni^{II}/Ti^{IV} = Ni^{II}/Ti^{IV}$	72.6	19.1		2.7		5.5

[a] M refers to the coating metal (Pd, Ag, Au, or Ni), while MO refers to the oxide of the coating metal (PdO, Ag_2O, Au_2O_3, or NiO).

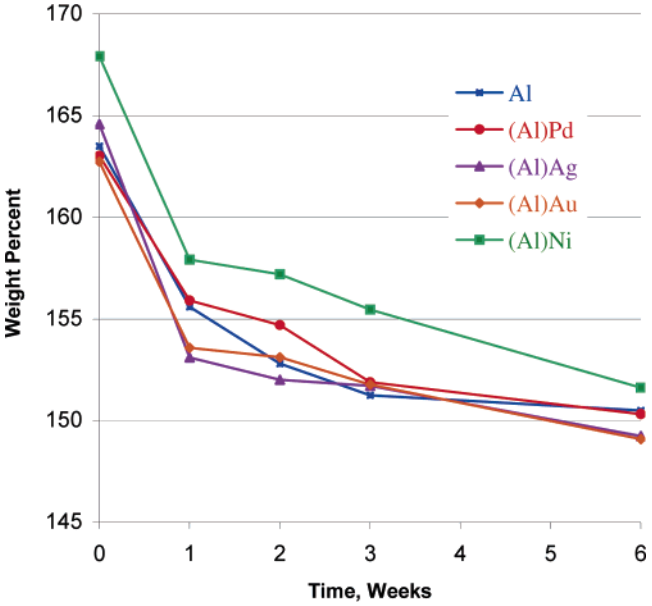

Figure 5. Aging of metal-coated powder samples at 85% relative humidity and room temperature. The weight increase upon complete oxidation is from TGA data, with the data for 0 weeks taken from the data in Figure 3.

The high active aluminum contents of the metal-coated samples result from a reduction in the amount of aluminum oxide (see Table 2), indicating that the coating metal is contributing to the passivation of the underlying aluminum metal. For Pd, Au, and Ag coatings the aluminum oxide content is reduced by roughly 4% compared to the untreated material, while for Ni coating the reduction is roughly 7%, equating to about a 25% relative reduction in aluminum oxide. The extent of reduction in aluminum oxide content is roughly proportional to the mole percent of coating metal. Perhaps surprising is the result that a small amount of Ni/NiO coating on the surface of the particle leads to a barrier to oxidation that equals or surpasses the effectiveness of aluminum oxide on a weight basis.

Currently, it is not known why the nickel treatment provides more active aluminum in the sample relative to the untreated material or samples treated with other metals. It is expected that an intermetallic material forms between the aluminum and nickel and plays a role in the behavior but cannot be counted on for a full explanation as palladium also participates in the formation of like compounds. Further investigation is warranted to determine what other metals may provide such a benefit and how they are related.

3.6. Aging at High Humidity. To determine the resistance to corrosion in an aggressive atmosphere, the samples were kept at 85% relative humidity at room temperature for several weeks. The weight gain upon oxidation in the TGA experiment was recorded using the previously detailed heating profile (Figure 5). During the first week at high humidity the largest change in the particles was observed with a loss of 10% in weight gain due to oxidation/hydrolysis. The reduction of the percent weight gain moderates after the first week with the different samples approaching ~151% weight upon oxidation indicating an active metal content of ~57%. Loss of weight gain could equate to a thicker oxide layer that protects the remaining metal from decomposition. The nickel-coated material maintained a slightly higher active aluminum content compared to the untreated aluminum, indicating that the enhanced passivation continued to be effective during aging.

4. Conclusions

Reacting an aluminum nanopowder with nickel acetylacetonate before air passivation produces a material with an active aluminum content that is equal to or higher than that for an untreated sample that has been simply air passivated. On exposure to the ambient atmosphere, it is expected that some, if not all, of the deposited nickel oxidizes to NiO. This nickel/nickel oxide coating reduces the formation of aluminum oxide such that less oxide is needed to passivate the aluminum. This is somewhat surprising considering that aluminum oxide forms a very efficient passivating layer for Al, requiring only a few nanometers to inhibit oxidation of the otherwise extremely reactive metal. The Pd, Ag, and Au coatings did not afford a similar enhancement in the amount of active metal, due to the heavier weight of these metals. Observed effects for nickel treated materials may become even more significant with a decreased particle size, where there would be a proportionately higher amount of the passivating oxide layer. These materials are of interest not only for increased active aluminum content but also due to their enhanced energy content and potential for undergoing thermite or intermetallic reactions.

Acknowledgment. This work was supported by the Defense Threat Reduction Agency. We thank Gregory Ostrom for conducting the ICP-AES analysis, Meghan Hargrave-Thomas and Daniel Connor for conducting the SEM and EDS analysis, and Dan Bliss for conducting the powder X-ray diffraction analysis.

CM047931K